

## Supplementary Information

### **Trapping lithium polysulfides of a Li-S battery by forming lithium bonds in a polymer matrix**

Kyusung Park<sup>1</sup>, Joon Hee Cho<sup>2</sup>, Ji-Hoon Jang<sup>1</sup>, Byeong-Chul Yu<sup>1</sup>, Andrea T. De La Hoz<sup>3</sup>, Kevin M. Miller<sup>3</sup>, Christopher J. Ellison<sup>1,2</sup>, and John B. Goodenough<sup>1\*</sup>

<sup>1</sup>Texas Materials Institute and <sup>2</sup>McKetta Department of Chemical Engineering, The University of Texas at Austin, Austin, TX 78712, United States

<sup>3</sup>Department of Chemistry, Murray State University, Murray, KY 42071, United States

\*Corresponding author. E-mail: [jgoodenough@mail.utexas.edu](mailto:jgoodenough@mail.utexas.edu)

## Synthesis of Vinyl Sulfone Monomer.

Preparation of 1,6-bis(vinylsulfone)hexane was completed by the following method.

### *Synthesis of 2,2'-(hexane-1,6-diylbis(sulfaneydiyl))diethanol 1:*

To a 1-L round-bottomed flask was charged powdered KOH (5.98 g, 1.06 mol) and 2-mercaptoethanol (9.61 g, 1.23 mol) in absolute ethanol (150 mL). To this stirred mixture was added dropwise a solution of 1,6-dibromohexane (10.0 g, 0.41 mol) in absolute ethanol (50 mL) at 0 °C. Once the addition was completed, the reaction was warmed to room temperature and allowed to stir for 30 minutes, followed by warming the reaction to 55 °C where it was held for 16 hours. The reaction was then cooled to room temperature and 5 % NaCl solution was then added to the reaction flask. The resulting solution was then concentrated *in vacuo* to remove the ethanol. To the resulting liquid was transferred to a separatory funnel and CH<sub>2</sub>Cl<sub>2</sub> was added. The organic phase was separated, washed three times with DI H<sub>2</sub>O and brine, dried over Na<sub>2</sub>SO<sub>4</sub>/MgSO<sub>4</sub>, filtered and the solvent removed under reduced pressure to afford 9.44 g of a white solid upon cooling (97 %). <sup>1</sup>H NMR (400 MHz, CDCl<sub>3</sub>): δ 1.34 (m, 4 H), 1.53 (m, 4 H), 2.47 (t, *J* = 7.3 Hz, 4 H), 2.65 (t, *J* = 6.3 Hz, 4 H), 2.81 (s, 2 H, -OH), 3.65 (t, *J* = 6.2 Hz, 4 H).

### *Synthesis of 2,2'-(hexane-1,6-diyldisulfonyl)diethanol 2:*

To a 500-mL round-bottomed flask was charged 2,2'-(hexane-1,6-diylbis(sulfaneydiyl))diethanol **1** (5.00 g, 21.0 mmol), Oxone® (38.73 g, 63.0 mmol) and absolute ethanol (200 mL). The resulting stirred mixture was warmed to 60 °C and held for 24 hours. The reaction was then filtered warm and the ethanol removed under reduced pressure. The residue was dissolved in DI H<sub>2</sub>O (200 mL) and extracted with EtOAc (4 x 200 mL). The organic extracts were combined, dried over Na<sub>2</sub>SO<sub>4</sub>/MgSO<sub>4</sub>, filtered and the solvent removed under reduced pressure to afford 4.07 g of a white solid (64 %). <sup>1</sup>H NMR (400 MHz, DMSO-*d*<sub>6</sub>): δ 1.39 (m, 4 H), 1.68 (m, 4 H), 3.09 (t, *J* = 7.1 Hz, 4 H), 3.18 (t, *J* = 6.0 Hz, 4 H), 3.77 (t, *J* = 6.0 Hz, 4 H), 4.01 (b s, 2 H, -OH).

### *Synthesis of 1,6-bis(vinylsulfonyl)hexane 3:*

To a 250-mL round-bottomed flask under nitrogen was dissolved 2,2'-(hexane-1,6-diyldisulfonyl)diethanol **2** (2.20 g, 7.27 mmol) and methanesulfonyl chloride (2.08 g, 18.19 mmol) in anhydrous dioxane (70 mL). To this stirred solution was added a solution of trimethylamine (7.36 g, 72.7 mmol) in anhydrous dioxane (20 mL) dropwise at room temperature using an addition funnel. After the addition was completed, the resulting solution stirred for 24 hours at room temperature and then the solvent was removed under reduced pressure. The resulting light brown oil was dissolved in DI H<sub>2</sub>O (120

mL) and extracted with  $\text{CH}_2\text{Cl}_2$  (3 x 70 mL). The organic extracts were combined, dried over  $\text{Na}_2\text{SO}_4/\text{MgSO}_4$ , filtered and the solvent removed under reduced pressure to afford a light brown oil, which was further purified using column chromatography with a gradient elution of 20-70 % EtOAc in hexanes. Purification (after solvent removal under reduced pressure) resulted in 1.40 g of an off-white solid (72 %).  $^1\text{H NMR}$  (400 MHz,  $\text{CDCl}_3$ ):  $\delta$  1.46 (m, 4 H), 1.80 (m, 4 H), 2.95 (t,  $J = 7.1$  Hz, 4 H), 6.15 (d,  $J = 10.1$  Hz, 2 H), 6.42 (d,  $J = 16.5$  Hz, 2 H), 6.60 (q, 2 H).

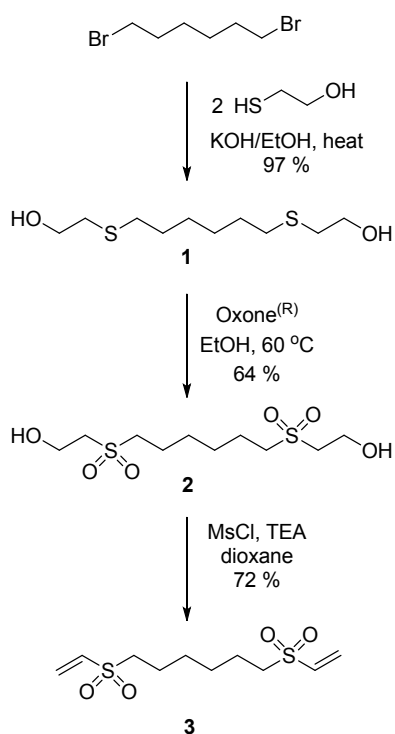
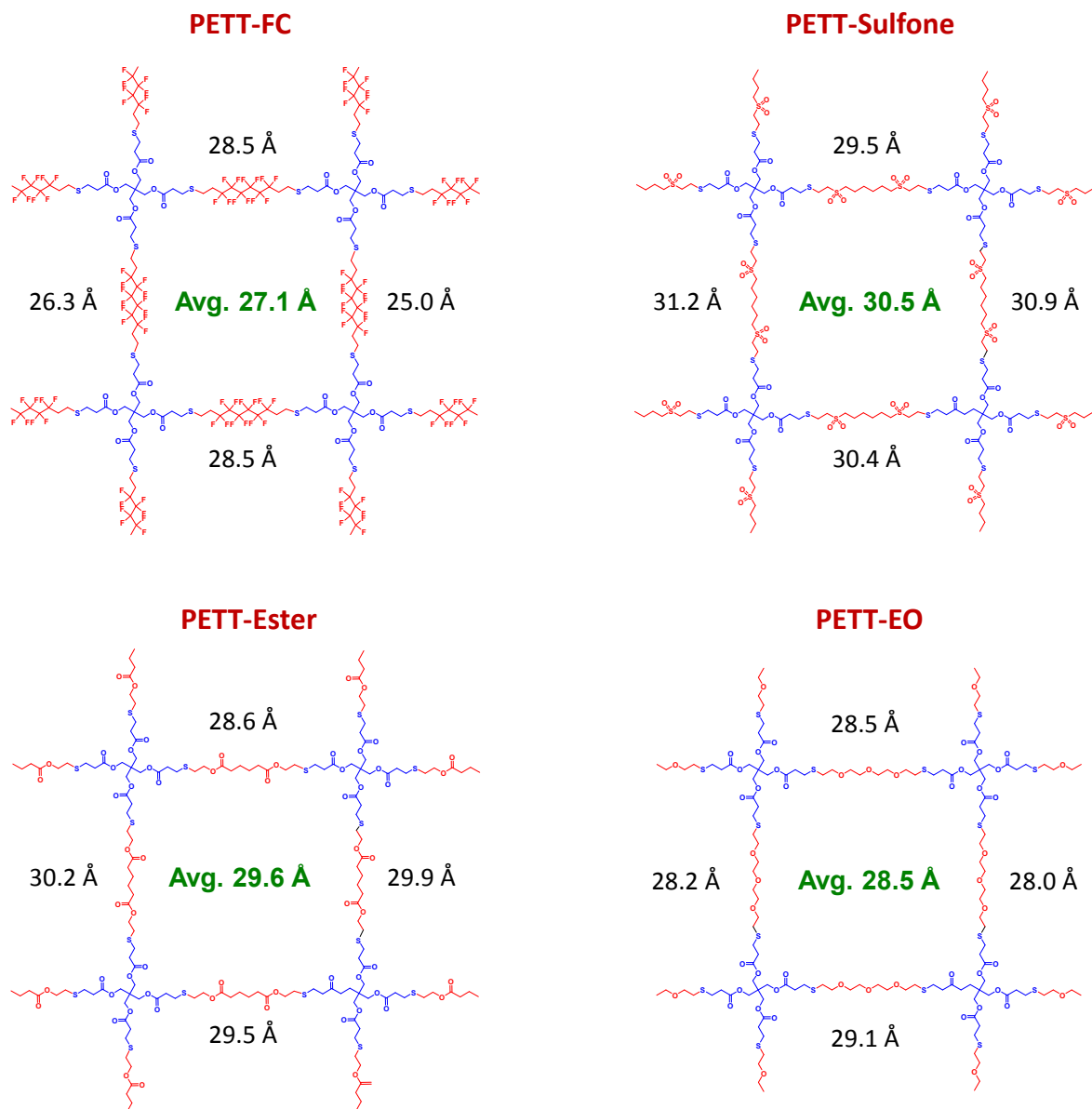


**Figure S1.** Calculated distances between crosslinks in PETT-FC, PETT-EO, PETT-Ester, and PETT-Sulfone.



## Discussion of the ATR-FTIR data in Fig. 1c

All spectra were normalized by the  $1730\text{ cm}^{-1}$  band that was assigned to the C=O vibration (See Table S1 for the detailed band assignments.). Ene ( $1620\text{-}1680\text{ cm}^{-1}$ ) and thiol ( $2550\text{-}2600\text{ cm}^{-1}$ ) bands do not appear in the infrared spectra of all the membranes, which indicates that most of the enes and thiols participated in the reaction and were completely depleted during the polymerization, which is ideal for preventing any electrochemical side reactions with residual monomers.

In the comparison of PETT-Ester and PETT-EO networks in Fig. 1c, the EO moieties are replaced with two esters and a  $\text{C}_4\text{H}_8$  aliphatic chain as shown in Fig. 1b, which caused an increased carbonyl stretching vibration peak at  $1730\text{ cm}^{-1}$  and the reduced the C-O-C absorbance around  $1100\text{ cm}^{-1}$ . As a result, the ratio of C=O to C-O-C vibration peak intensities was reversed between the PETT-EO and PETT-Ester membranes.

Fig. 1c also compares the ATR-FTIR spectra of PETT-EO and PETT-Sulfone. Compared to PETT-EO, PETT-Sulfone bears sulfones and  $\text{-(CH}_2\text{)}_6\text{-}$  chains instead of the EO groups. The sulfone band ( $1140\text{ - }1170\text{ cm}^{-1}$ ) is overlapped with the EO peak ( $1050\text{ - }1150\text{ cm}^{-1}$ ), but a strong rocking adsorption of  $\text{-(CH}_2\text{)}_6\text{-}$  can be found centered at  $750\text{ cm}^{-1}$ , demonstrating the different chemical structure of these two networks.

For PETT-FC in Fig. 1c, a broad peak at approximately  $2900\text{ cm}^{-1}$  on the PETT-FC curve, associated with  $\text{CH}_2$  asymmetric/symmetric stretching absorption, is smaller than that of PETT-EO. This relation is due to the substitution of perfluorocarbons for ethylene oxides. The C-F vibration and ether absorbance peaks overlap one another approximately in the frequency range of  $1100\text{ - }1200\text{ cm}^{-1}$ , but a significant intensity increase in PETT-FC should reflect the higher density of perfluorocarbons than that of EO in the polymer backbones.

**Table S1. Assignments of ATR-FTIR spectra of the synthesized crosslinked networks.**

Origin	Group frequency, wavenumber (cm <sup>-1</sup> )	Measured wavenumber (cm <sup>-1</sup> )	Assignment
C-H	2915-2935 / 2845-2865	2930 / 2860	Methylene C-H asym./sym. stretch
	720-750	733-748	Methylene -(CH <sub>2</sub> ) <sub>n</sub> - rocking (n ≥ 3)
C=O	1725-1750	1730	Ester
C-O-C	1050-1150	1100	Alkyl-substituted ether, C-O stretch
O=S=O	1140-1170	1130	Sulfones, SO <sub>2</sub> sym. stretch
C-F	1000-1150	1140	Aliphatic fluoro compounds, C-F stretch
Thiol	2550-2600	Not detected	Thiols, S-H stretch
-Ene	1620-1680	Not detected	Alkenyl C=C stretch

Coates, J. Interpretation of Infrared Spectra, A Practical Approach. In *Encyclopedia of Analytical Chemistry*, Meyers, R. A. (Ed.); John Wiley & Sons Ltd.: Chichester, 2000; pp. 10815-10837

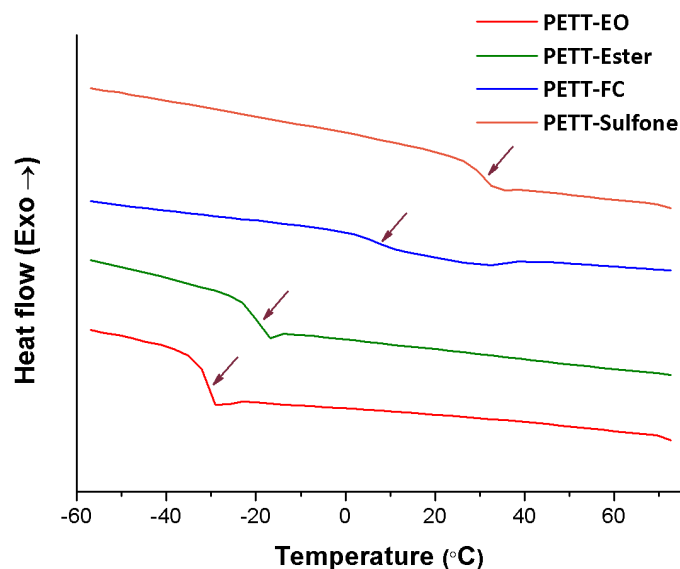


**Figure S2.** Differential scanning calorimetry (DSC) thermograms of PETT-EO, PETT-Ester, PETT-FC, and PETT-Sulfone membranes, recorded during the second heating cycle.  $T_g$  is indicated by an arrow for each sample.

**Note.** PETT-EO and PETT-Ester thiolene networks exhibited a  $T_g$  at  $-30.9\text{ }^\circ\text{C}$  and  $-19.9\text{ }^\circ\text{C}$ , temperatures well below room temperature. In parallel, PETT-FC showed a major  $T_g$  at  $6.3\text{ }^\circ\text{C}$  and a following broad endothermic “mound” ranging up to  $38\text{ }^\circ\text{C}$ , likely associated with multiple glass transitions. Gradual evaporation of THF during the polymerization could, due to the hydrophobic nature of fluorocarbons, cause minor phase separation of perfluorocarbon in the solution. The phase separations might result in multiple glass transitions, derived from minor molecular heterogeneity in the resultant network, around the main  $T_g$ . On the other hand, the  $T_g$  of PETT-Sulfone was  $30.8\text{ }^\circ\text{C}$ , above room temperature, which could reduce the amount of the electrolyte uptake at room temperature. An endothermic peak corresponding to a  $T_m$  and the associated crystallization peak were not observed for any polymer membranes. However, unquantifiable weak glass transition signals were shown around  $80\text{ }^\circ\text{C}$  for PETT-EO, PETT-Ester, and PETT-Sulfone, suggesting these polymer networks were predominantly homogeneous and in their fully amorphous phase. It may be reasonably deduced that the highly uniform and dense crosslinking between vinyl monomers and thiols with small molecular weights would efficiently suppress crystallization within the networks.

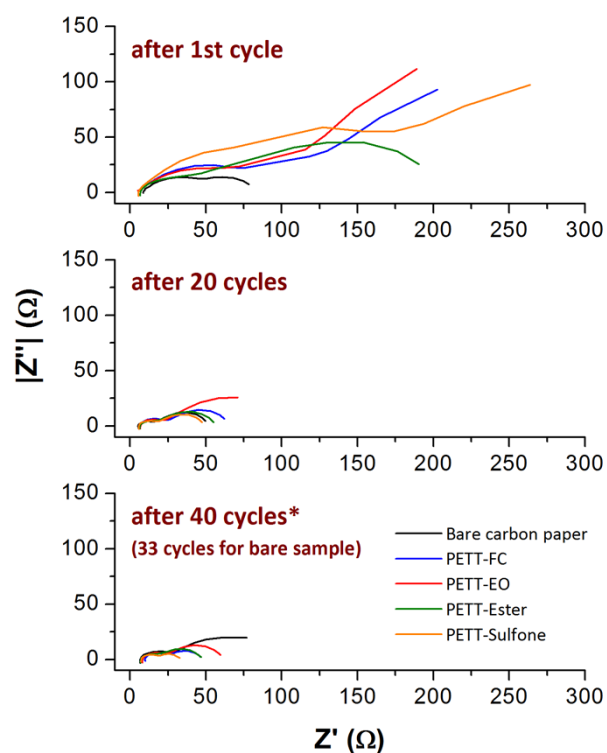


**Figure S3.** Nyquist plots for the bare carbon paper electrode, PTT-FC, PTT-EO, PTT-Ester, and PTT-Sulfone after the 1<sup>st</sup>, 20<sup>th</sup>, and 40<sup>th</sup> cycles. For the bare carbon electrode, it was terminated after the 33<sup>rd</sup> cycle owing to the endless shuttle current and characterized. After the designated number of cycles, the coin cells were investigated for electrochemical impedance spectroscopy (1260A, Solartron) from 1 MHz to 0.1 Hz with an AC voltage amplitude of 20 mV.

**Note.** In the Nyquist plots, the first and second depressed semicircles were assigned to the SEI component and the charge-transfer resistance, respectively. It was noted after the first cycle that unlike the low impedance in the bare carbon electrode, the polymer-coated electrodes showed higher charge-transfer resistance. However, after the initial cycles (e.g. 20 cycles), the impedance values were significantly reduced and became comparable to that of the bare carbon electrode. The resistance change during cycling corresponds well to the charge/discharge characteristics in Fig. 2c. Further cycling also slightly reduces the resistance values. It should also be noted that the bare carbon electrode that terminated after 33 cycles owing to the endless charging current still shows a low charge-transfer resistance. This result suggests that a cell degradation by the polysulfide shuttle phenomenon does not necessarily increase the cell impedance significantly. Finally, it should be pointed out that the difference in the impedance values between the different polymers cannot solely explain the charge/discharge behaviors in Fig. 2.